

Realistic Nuclear Single-Particle Hamiltonians and the Proton Shell 114†

HEINER MELDNER*

Lawrence Radiation Laboratory and Department of Physics, University of California, Berkeley, California 94720

(Received 15 October 1968)

A simple *self-consistent* single-particle equation is investigated and compared with similar attempts. The proposed model is designed to be particularly suitable for the calculation of (adiabatic) fission processes. The kernel of this integrodifferential equation has a structure that allows satisfactory reproduction, with one constant set of five physical parameters, of (1) charge density distributions, including isotope shifts, (2) $1s$ proton levels as measured in $(e, e'p)$ scattering, (3) total binding energies or nuclear mass defects, and (4) the shell-model spin assignments and mass structure throughout the periodic table. Hence, it seems that all future work in this direction has to confirm *quantitatively* the essential features determined here, particularly the *nonlocality* and *rearrangement* effects. Rearrangement energies appear explicitly, since the present model, like self-consistent fields of appropriate many-body formalisms, yields different eigenvalue spectra and mass defects for different occupation functions. The partial derivative $\partial E/\partial Z$ of the total binding energy (mass) changes considerably at the proton number $Z=114$ when the present Hamiltonian is used for superheavy nuclei. This confirms an earlier suggestion made by this author on the basis of a gap in the proton eigenvalue spectrum at $Z=114$. The present calculations show that this shell effect becomes insignificant for isotopes too far from the extrapolated β stability line, in particular for $N \lesssim 172$.

INTRODUCTION

PHENOMENOLOGICALLY, the Hamiltonian for a nucleon bound in a nucleus allows a rapidly converging expansion: $H = H_1 + H_2 + \dots$ in terms of one-body, two-body, etc., operators; i.e., a "realistic" model for the single-particle Hamiltonian H_1 accounts rather accurately for gross nuclear data of bound and scattering states, thus leaving only small phenomenological many-body forces to produce residual correlations. This picture allows comprehension of essential facts such as the pronounced nuclear shell structure and the extremely small ratio of the odd-even mass staggerings to the nuclear binding energies. However, even a dozen years after the establishment of the shell-model phenomenology,¹⁻³ basic *quantitative* questions, about the extent of *nonlocality* of H_1 and its *rearrangement*-type response, e.g., are far from being incontrovertibly settled.

One purpose of this work is to investigate such features of realistic nuclear single-particle Hamiltonians without the usual restrictions and oversimplifications caused by limited computer facilities. For example, self-consistent equations with nonlocal potentials are solved (numerically) exactly here.

Two approaches for the determination of H_1 are easily distinguished: Number one is the direct pragmatic way, i.e., an ansatz for a phenomenological single-particle equation (usually involving nonlocal one-body potentials). The second deploys some

many-body formalisms with phenomenological two-body potentials. At the present stage of the theory, a preference for the latter is unfortunately based on the prejudice that a complicated answer to a complicated question is more reliable than a simple one. This uncertainty is due to the fact that all approaches of the second kind, although potentially closer to a first-principle method, still have to be based on a practically unsolved many-hadron problem. The NN interaction is not sufficiently understood at the distances of major importance for this purpose, i.e., smaller than half the inverse pion mass.⁴ This implies the high uncertainty in the off-energy-shell behavior of NN potentials,⁵ particularly in their nonlocality. The nonlocality quite obviously exhibits the ambiguity of fits of the two-body NN scattering with potential models, since one can always construct classes of phase-shift equivalent potentials with identical spectra but quite different off-energy-shell behavior, including cases which give singular Hartree-Fock-type matrix elements; e.g., any unitary transformation acting on a given two-body Hamiltonian that contains some NN phase-shift-fitting potential gives another Hamiltonian, such as $e^{i\Omega} H e^{-i\Omega}$, usually with a potential of different nonlocality or off-energy-shell behavior. The fit to the on-shell data is preserved, as long as the change of the T matrix (proportional to the change of the Hamiltonian⁶) vanishes there, i.e., $\delta T \sim \delta H \sim [\Omega, H] = 0$. Thus, all such transformations with Hermitian two-body operators Ω yield equivalent on-shell potentials once the transition matrix element of this commutator vanishes.⁷ This can be viewed as a formal method of

† Work was performed under the auspices of the U.S. Atomic Energy Commission while the author was holding a NATO postdoctoral fellowship.

* Present address: Freie Universität Berlin, West-Berlin, Germany.

¹ M. G. Mayer and J. H. D. Jensen, *Elementary Theory of Nuclear Shell Structure* (John Wiley & Sons, Inc., New York, 1955); D. H. Wilkinson, *Comment Nucl. Part. Phys.* **II**, 48 (1968); **II**, 83 (1968).

² H. A. Bethe, *Phys. Rev.* **103**, 1353 (1956).

³ K. A. Brueckner, *Phys. Rev.* **97**, 1353 (1955).

⁴ Cf. E. Lomon and H. Feshbach, *Rev. Mod. Phys.* **39**, 611 (1967).

⁵ Cf. H. Pierre Noyes, Saclay Conference paper No. SLAC-PUB-256, 1967; I am indebted to Professor Noyes for enlightening discussions on these problems.

⁶ Cf. M. L. Goldberger and K. M. Watson, *Collision Theory* (John Wiley & Sons, Inc., New York, 1955).

⁷ P. Mittelstaedt and M. Ristig, *Z. Physik* **193**, 349 (1966); see also, G. A. Baker, *Phys. Rev.* **128**, 1485 (1962).

obtaining families of equivalent potentials by generalized Scott-Moszkowski-type⁸ separations. Therefore, it would seem futile to work numerically with the second approach, as long as the question of off-energy-shell behavior is not sufficiently understood *quantitatively*. At present, it is hardly possible to make even the qualitative decision between the extreme cases of purely local hard-core versus highly nonlocal smooth potentials.⁹

It seems safe, however, to adopt as a basis a non-relativistic potential description of NN forces at the low kinetic energies of nucleons bound in many-baryon systems. This belief is due to the small ratio of the pion to the nucleon mass.¹⁰ Thus, it is also safe to rely on the gross structure of single-particle equations as given by many-body formalisms and approximations which are based on sufficiently general NN potentials. This—presently wise—restriction on the *qualitative* results of such formalisms requires the parametrization of a nuclear single-particle Hamiltonian, as is done, e.g., via the ansatz of a Woods-Saxon or Nilsson-type potential, usually with some velocity dependence.^{11–14} However, these simple models of a nuclear self-consistent field can be replaced now. Modern computers allow a considerably improved simulation of the nuclear single-particle equations that are expected from reasonable many-body formalisms.

One suggestion in this direction is made here (Sec. 1). Complications actually required are slight in comparison to those necessary for the ancient nuclear-well ansatz. The proposed single-particle Hamiltonian has a structure close to the one given grossly by Hartree-Fock-Bogolubov or Brueckner-type formalisms, i.e. nonlocality, density, spin-orbit, and isospin dependences are introduced into the kernel of this equation in the form expected in first order from such formalisms involving rather general nonlocal NN potentials.

Section 2 A shows that only five physical parameters allow a surprisingly good fit to many independent data throughout the periodic table. Such a widespread application was inconceivable with previous models of H_1 . The essential features of a realistic single-particle Hamiltonian seem to be determined rather uniquely this way. They will have to be confirmed once substantial experimental information on the off-energy-shell be-

⁸ S. A. Moszkowski and B. L. Scott, *Ann. Phys. (N.Y.)* **11**, 65 (1960).

⁹ Cf., for example, the discussion in *Proceedings of the International Conference on Nuclear Physics, Gallinburg, Tennessee, 1967* (Academic Press Inc., New York, 1967), p. 673.

¹⁰ Cf. G. Chew, *Phys. Rev. Letters* **19**, 1492 (1967); *Comments Nucl. Part. Phys.* **II**, 107 (1968).

¹¹ H. Meldner and G. Suessmann, *Phys. Letters* **6**, 353 (1963).

¹² A. A. Ross, R. D. Lawson, and H. Mark, *Phys. Rev.* **104**, 401 (1956); P. E. Nemirowsky, *Zh. Eksperim. i Teor. Fiz.* **36**, 889 (1959) [English transl.: *Soviet Phys.—JETP* **9**, 627 (1959)]; D. J. Wyatt, J. G. Wills, and A. E. S. Green, *Phys. Rev.* **119**, 1031 (1960); L. R. B. Elton and A. Swift, *Nucl. Phys.* **A94**, 52 (1967).

¹³ H. Meldner, *Arkiv Fysik* **36**, 593 (1967).

¹⁴ C. Gustafson, I. L. Lamm, B. Nilsson, and S. G. Nilsson, *Arkiv Fysik* **36**, 613 (1967).

havior of NN potentials has been accumulated so that some number two approaches can leave the status of model-dependent models. The quantitative results of the fairly conservative and pragmatic approach adopted here provide a rather safe foundation. This resembles the situation in nuclear physics of *small*-baryon-number hadron systems, where a pragmatic approach now determines basic features in terms of Regge singularity parameters.

Rearrangement-type responses (Sec. 3) of this self-consistent model appear to have the right order of magnitude. Orbital rearrangement energies, for example, were found to be comparable to level spacings in nuclear potential wells.¹⁵ This result seriously questions the usual identification of such *level spacings* with the *mass differences* observed, e.g., in nucleon transfer reactions.

In the presence of fluctuating rearrangement energies, a gap in the eigenvalue spectrum, as, e.g., found at the proton number 114, does not necessarily lead to a real shell effect in the masses as a function of nucleon numbers. The deployment of this realistic Hamiltonian in the region of superheavy nuclei (Sec. 4) therefore provides an almost independent check on the magic proton number 114 which was originally^{13,14,16–18} suggested from extrapolations of proton eigenvalue spectra.

All data in this paper refer to spherical nuclei; Sec. 5 deals in some detail with the straightforward extension of this self-consistent field model to axially symmetric deformed densities. The present form has particular advantage for the description of adiabatic fission processes.

The Appendix is concerned with some of the computational problems.

1. SELF-CONSISTENT FIELD MODEL

A single-particle equation of the type

$$\left(\frac{\hbar^2}{2m} \frac{\partial^2}{\partial \mathbf{r}^2} - \epsilon_{\nu, m_i} \right) \varphi_{\nu, m_i}(\mathbf{r}) = \int d\mathbf{r}' K_{m_i}(\mathbf{r}, \mathbf{r}') \varphi_{\nu, m_i}(\mathbf{r}') \quad (1)$$

is sufficiently general to allow for a rather realistic model of the nuclear self-consistent field. The subscript ν stands for all quantum numbers specifying a bound nucleon except for its isospin 3-component m_i . The formalism for the plain Hartree(HF)-Fock calculation, for instance, viz.,

$$K_{m_i}^{\text{HF}}(\mathbf{r}, \mathbf{r}') = \sum_i \left[\varphi_i^*(\mathbf{r}) u(\mathbf{r}, \mathbf{r}') \varphi_i(\mathbf{r}') - \delta(\mathbf{r} - \mathbf{r}') \right. \\ \left. \times \int d\mathbf{x} \varphi_i^*(\mathbf{x}) u(\mathbf{x}, \mathbf{r}') \varphi_i(\mathbf{x}') \right] + \left(\frac{1}{2} - m_i \right) K_{\text{Coul}}, \quad (2)$$

¹⁵ H. Meldner, *Nuovo Cimento* **53B**, 195 (1968).

¹⁶ Cf. Ref. 23 in the paper of Myers and Swiatecki.

¹⁷ W. D. Myers and W. J. Swiatecki, *Nucl. Phys.* **81**, 1 (1966).

¹⁸ A. Sobiczewski, F. A. Gareev, and B. N. Kalinkin, *Phys. Letters* **22**, 500 (1966); S. G. Nilsson, J. R. Nix, A. Sobiczewski, Z. Szymanski, S. Wycech, C. Gustafson, and P. Möller, *Nucl. Phys.* **A115**, 545 (1968).

with suitable models for $u(\mathbf{r}, \mathbf{r}')$ provides nuclear single-particle Hamiltonians which are quantitatively almost as useful as the ones mentioned in the Introduction.¹⁹ Therefore, the HF result, i.e., the result in the limit where perturbation methods are applicable to more general many-body formalisms, is sometimes referred to in the following discussion—although one should by no means regard the phenomenological kernel proposed here as being necessarily connected with a plain HF formalism.

A comparison of (2) with the symmetrical factorized Van Vleck-type kernel²⁰

$$K_{m_i}(\mathbf{r}, \mathbf{r}') = v(|\mathbf{r}-\mathbf{r}'|)u_{m_i}(\mathbf{r}+\mathbf{r}') + (\frac{1}{2}-m_i)K_{\text{Coul}}, \quad (3)$$

yields upper bound estimates for the “ranges” of u and v ; namely, the range in $|\mathbf{r}-\mathbf{r}'|$ should not exceed the order of the inverse pion mass (1.4 fm) and the function u should essentially vanish for its argument larger than nuclear radii ($A^{1/3}$ fm). Therefore, u is usually taken to be proportional to the nuclear matter distribution. Lower limits on the range of the factor v are required, for instance, in order to reproduce the observed momentum dependence of local potential wells, i.e., the fact that the effective mass of bound nucleons is not larger than 0.5 in real nuclei^{3,21}. As is shown in the next section, this clearly *excludes* nonlocality ranges which are small enough to render a δ function for v , i.e., local potentials a reasonable ansatz. Since the factorized form (3) also allows for self-consistency, it would appear to yield the simplest kernel that has a chance to simulate any realistic nuclear self-consistent field.

A. Nonlocality

Figure 1 shows empirical information on the Fourier transform of $v(|\mathbf{r}-\mathbf{r}'|)$, i.e. the approximately equivalent (momentum)²-dependent local potential depth $\bar{v}(k^2)$, defined, e.g., through

$$\begin{aligned} \varphi\bar{v}(k^2) &= \int d\mathbf{r}' K(\mathbf{r}, \mathbf{r}')\varphi(\mathbf{r}') \\ &= \varphi u(0) \int d\mathbf{r}' \exp[i\mathbf{k}\cdot(\mathbf{r}-\mathbf{r}')]v(|\mathbf{r}-\mathbf{r}'|). \quad (4) \end{aligned}$$

¹⁹ K. T. R. Davies, S. J. Krieger, and M. Baranger, Nucl. Phys. **84**, 545, (1966); W. H. Bassichis, A. K. Kerman, and J. P. Svenne, Phys. Rev. **160**, 746 (1967); D. Vautherin and M. Vénéroni, Phys. Letters, **26B**, 552 (1968); P. Pirès, R. De Tourreil, D. Vautherin, and M. Vénéroni, in Proceedings of the 1968 International Symposium on Nuclear Structure, Dubna, USSR (unpublished); A. Faessler, P. U. Sauer, and H. H. Wolter, *ibid.*

²⁰ For some discussion on this particular choice see, e.g., W. E. Frahn and R. H. Lemmer, Nuovo Cimento **6**, 664 (1957); A. L. Fetter and K. M. Watson, in *Advances in Theoretical Physics I*, edited by K. A. Brueckner (Academic Press Inc., New York, 1965); A. E. S. Green, Rev. Mod. Phys. **30**, 569 (1958); K. A. Brueckner, Phys. Rev. **103**, 1121 (1956); J. H. Van Vleck, *ibid.*, **48**, 367 (1935).

²¹ M. H. Johnson and E. Teller, Phys. Rev. **98**, 783 (1955); V. F. Weisskopf, Nucl. Phys. **3**, 423 (1957); Rev. Mod. Phys. **29**, 174 (1957); K. A. Brueckner, A. M. Lockett, and M. Rotenberg, Phys. Rev. **121**, 255 (1961).

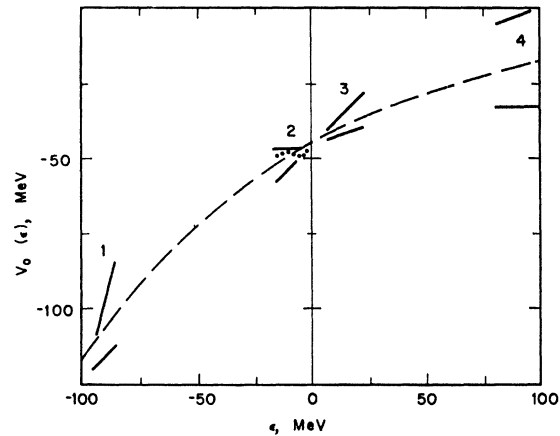


FIG. 1. Depth of the nucleon-nucleus potential as a function of energy. The solid bars give the limits for regions 1-4 as discussed in Sec. 1 A.

Therefore, in order to specify reasonably well a nonlocality function $v(|\mathbf{r}-\mathbf{r}'|)$, one needs in addition to its width in $|\mathbf{r}-\mathbf{r}'|$ at least one more property like its asymptotic slope. For example, Yukawa and Gaussian form factors $v(|\mathbf{r}-\mathbf{r}'|)$ fit the dashed curve in Fig. 1

$$v_0(\epsilon) = v(\epsilon - v_0(\epsilon)), \quad (5)$$

with widths around 0.8 and 1.5 fm, respectively (cf. Ref. 14). The most important evidence on $v_0(\epsilon)$ in region 1 comes from the $(e, e'p)$ experiments.²² The data on ⁴⁰Ca and ⁷⁵As suggest that 1s protons are bound by at least 80 MeV in heavier nuclei. Other limits on $v_0(\epsilon)$ in this region may be inferred from estimates of the effective nucleon mass in nuclear matter.^{3,21}

In region 2, i.e., for ϵ around the Fermi energies, $v_0(\epsilon)$ is most accurately determined in absolute magnitude—via the observed separation energies. But the slope there is subject to some speculations. One school suspects an appreciable wiggle there,²³ a zero, or even a sign change of the slope as indicated by the dotted line in Fig. 1. However, the arguments presented for such anomalies are not conclusive yet (cf. Sec. 3 and Ref. 15).

In regions 3 and 4 the evidence comes mainly from fits of nucleon-nucleus scattering.²⁴⁻²⁸ Although one cannot completely disentangle the energy dependences of real and imaginary parts, there is general agreement

²² For results on ⁷⁵As, see U. Amaldi, Jr., G. C. Venuti, G. Cortellessa, E. De Sanctis, S. Frullani, R. Lombard, and P. Salvadori, Accad. Naz. Lincei-Rend. Sc. fis. mat. e nat. Serie VIII, **XLI**, fasc. 6 (1966) for results on ⁴⁰Ca, Phys. Letters **22**, 593 (1966).

²³ G. E. Brown, J. H. Gunn, and P. Gould, Nucl. Phys. **46**, 598 (1963).

²⁴ P. E. Hodgson, *The Optical Model of Elastic Scattering* (Oxford University Press, New York, 1963).

²⁵ F. G. Perey and B. Buck, Nucl. Phys. **32**, 353 (1962); H. Schulz and H. Wiebicke, Phys. Letters **21**, 190 (1966).

²⁶ L. Rosen, J. G. Beery, A. S. Goldhaber, and E. H. Auerbach, Ann. Phys. (N.Y.) **34**, 96 (1965); R. L. Cassola and R. D. Koshel, Nuovo Cimento **53B**, 363 (1967).

²⁷ F. G. Perey, Phys. Rev. **131**, 745 (1963).

²⁸ Cf., for example, A. Watt, Phys. Letters **27B**, 190 (1968).

TABLE I. The two parameter sets used in the present calculation. Except for Table II all results refer to parameter set A.

	v (MeV)	a (fm)	ρ_1 (fm ⁻³)	σ (fm ²)	τ
Set A	391.3	0.8	0.3	0.5	0.3
Set B	289.0	0.9	0.4	0.5	0.3

now that the real part has the minimum decrease, with energy indicated in Fig. 1 for the well-analyzed 10-MeV region. Straightforward use of the real part of an optical-model fit did exactly yield the shell structure.¹¹ However, the nonlocality there did correspond to the lower limit for the slope indicated in region 3 (derived from Refs. 25 and 26) and gave only about half the total binding energy.²⁹ Therefore, the stronger energy dependence indicated by other optical-model fits²⁷ is favored from the bound-state fits—if one excludes a strong curvature of $v_0(\epsilon)$ for $\epsilon \lesssim 0$. No appreciable energy dependence is established for the 100-MeV region; v_0 may essentially become a constant there.^{24,28}

The dashed curve in Fig. 1 corresponds to a Yukawa nonlocality function with the width used here (cf. set A of Table I). This simple form can account quite well for the data. Superpositions of several Yukawas that did, for instance, give a wiggle in region 2 were found to be unnecessary at this stage of the phenomenology. A Yukawa, i.e., an NN potential-type function is suggested from the Van Vleck kernel and seems to fit the curvature in Fig. 1 a little better than a Gaussian.

B. Saturation and Density Dependence

The real part of u in Van Vleck-type kernels is usually taken to be similar to the matter density ρ .^{20,26} Taking literally $u = \rho(\frac{1}{2}(\mathbf{r} + \mathbf{r}'))$ is, of course, not consistent: The output ρ from a bound-state calculation has a smaller rms radius than the input. This self-consistency problem can be solved by adding to the width function v , the “interaction” in the Van Vleck kernel, some density dependence such as

$$v(\mathbf{r} - \mathbf{r}') [1 - \alpha \rho^\beta (\frac{1}{2}(\mathbf{r} + \mathbf{r}')) - \dots], \quad (6)$$

with $\alpha, \beta > 0$. The resulting kernel $\sim v(1 - \alpha \rho^\beta)$ gives a sum of terms proportional to $\rho^{2/3}$, $-\rho$, and $\rho^{1+\beta}$ for the energy—readily seen from the Thomas-Fermi approximation. One can therefore make it stationary at the observed nuclear saturation densities. In this class is, for instance, Bethe's recent proposal for the effective NN interaction³⁰: $v(1 - \alpha \rho^{2/3})$. A similar term appears in

²⁹ R. D. Koshel, Phys. Rev. **144**, 811 (1966).

³⁰ H. A. Bethe in *Proceedings of the International Conference on Nuclear Physics, Gallinburg, Tennessee, 1967* (Academic Press Inc., New York, 1967); see also A. Lande and J. P. Svenne, Phys. Letters **25B**, 91 (1967); and A. M. Green, Phys. Letters **24B**, 384 (1967). Introducing this term as an explicit density dependence of the two-body potential would modify the relation used here [Eq. (18)] for the total binding energy. I am grateful to Professor K. A. Brueckner for discussions on these questions.

HF-type formalisms as a first-order correction for nonlocality of the two-body potential. This is seen from the analogous formula to Eq. (4) for a nonlocal NN potential. The equivalent momentum-dependent potential derived in this way is a local one multiplied by the usual power series in momentum operators squared—if the kernel is symmetric:

$$v(1 - ap^2 - bp^4 - \dots); \quad (7)$$

and Eq. (6) follows from the statistical approximation $p \sim p^{1/3}$. The particular power β is therefore suggested from such considerations and used in the model below. The choice is not critical as long as $\beta = \frac{2}{3}$ is not very different from this value. Some variations in the range $0.3 \leq \beta \leq 1$ with adjustments of other parameters left results practically unchanged.

Similar arguments hold for the simplification of taking $\rho(\frac{1}{2}(|\mathbf{r}| + |\mathbf{r}'|))$ instead of $\rho(\frac{1}{2}(\mathbf{r} + \mathbf{r}')) = \rho(\frac{1}{2}(|\mathbf{r} + \mathbf{r}'|))$ for the spherical density distributions considered here (for nonspherical ρ see Sec. 5). Both choices should give essentially the same fits to the data up to some parameter renormalization.

A summation of the preceding considerations therefore yields as the most straightforward model of a nuclear kernel:

$$K(\mathbf{r}, \mathbf{r}') = v(|\mathbf{r} - \mathbf{r}'|) \{1 - [\rho(x)/\rho_1]^{2/3}\} \rho(x), \\ x = \frac{1}{2}(|\mathbf{r}| + |\mathbf{r}'|). \quad (8)$$

This will be adorned by two “fine-structure” terms discussed in Secs. 1 C and 1 D.

C. Isospin Dependence

Conventionally, the isospin dependence of nuclear single-particle Hamiltonians is introduced via a Lane potential³¹

$$\mathbf{t} \cdot \mathbf{T} / A, \quad (9)$$

where \mathbf{t} and \mathbf{T} are, respectively, the isospins of the nucleon and residual nucleus in question. However, this term yields the wrong isotopic variation of rms radii of, e.g., Ca isotopes if it is used with the strength necessary in optical-model fits or as required to fit the neutron/proton ratio in heavy nuclei. Only an inconsistently small strength parameter could reproduce the data.³²

Considerations similar to the ones that led to the kernel (8) would suggest the use for the effective ρ of an appropriately weighted average of the densities $\rho_{(\pm 1/2)}$ corresponding to neutrons and protons, namely,

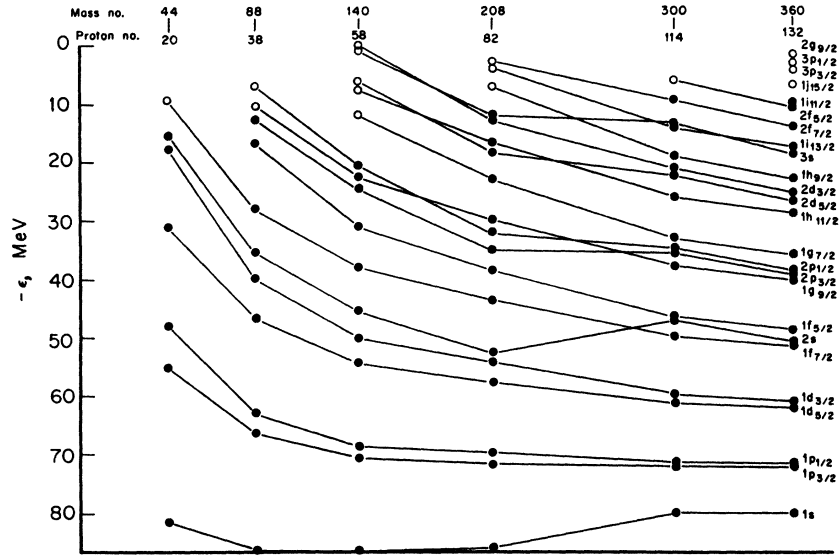
$$\rho_{m_i} \sim \rho_{(-m_i)} + \tau \rho_{(m_i)} \quad (10)$$

with a dimensionless parameter $\tau < 1$. This can be interpreted as assuming that only a fraction of the like nucleons interact with the particle in question, or that

³¹ A. M. Lane, Nucl. Phys. **35**, 676 (1962).

³² B. F. Gibson and K. J. van Oostrum, Nucl. Phys. **90A**, 159 (1967); cf. also A. Swift and L. R. B. Elton, Phys. Rev. Letters **17**, 484 (1966).

FIG. 2. Proton eigenvalue spectra for spherical nuclei close to the line of β stability. Eigenvalues with equal quantum numbers are connected by straight lines (to guide the eye). Note the somewhat fluctuating results as compared to the smooth curves of non-self-consistent calculations (Ref. 13).



they are felt by the particle to be as attractive as the unlike ones. One can therefore account for effects of the Pauli principle as well as for isospin-dependent terms in the NN interaction. It is only the latter that led to the assumption of the Lane potential. In the statistical limit, where surface terms are neglected, a simple exercise shows the present ansatz (10) to be completely equivalent to Lane's term $\rho(1+\alpha\mathbf{t}\cdot\mathbf{T}/A)$. However, Eq. (10) can reproduce satisfactorily the neutron/proton ratios or optical-model results as well as the isotope shifts in rms radii. Recent fine-structure investigations of the isospin dependence³³ also seem to favor a term like (10).

D. Spin-Orbit Interaction

A single-particle spin-orbit term of the type

$$\mathbf{s}\cdot\mathbf{l}r^{-1}(d\rho/dr) \quad (11)$$

can be derived from HF-type formalisms³⁴ and now even its strength appears to be understood in this framework.³⁵ About equally satisfactory seems to be the pragmatic introduction of this term as the simplest invariant (with respect to rotations and inversions) proportional to \mathbf{p} , \mathbf{s} , and $\nabla\rho$, namely,³⁶ $(\mathbf{p}\times\mathbf{s})\cdot\nabla\rho$. This gives Eq. (11) for spherical nuclei. However, the present calculations with such a term did not show very clearly the shell structure for heavy nuclei, as seen, e.g., from the results of Sec. 2. One reason seems to be the factor $r^{-1}d\rho/dr$ which emphasizes the influence of wiggles in the inside density distribution. This did not

show up in similar but non-self-consistent models where the density (or potential) was proportional to the usual Fermi function which is practically constant inside. Therefore, a form

$$r^2(\mathbf{p}\times\mathbf{s})\cdot\nabla\rho \quad (12)$$

might improve the results.

2. PARAMETRIZATION

A. Five-Parameter Kernel

The accumulation of all essential pieces from Sec. 1 yields the five-parameter kernel

$$K_{m_t}(\mathbf{r}, \mathbf{r}') = ve^{-v|\mathbf{a}|/(y/a)} [1 - (\rho_{m_t}(x)/\rho_1)^{2/3}] \times [1 - (\sigma/x)\mathbf{s}\cdot\mathbf{l}(d/dx)] \rho_{m_t}(x) + \delta(y) [\frac{1}{2} - m_t] V_{\text{Coul}}(x), \quad (13)$$

with

$$\rho_{m_t} = [\rho_{(-m_t)} + \tau\rho_{(m_t)}] (1+\tau)^{-1},$$

$$x = \frac{1}{2}(r+r'), \quad y = |\mathbf{r}-\mathbf{r}'|,$$

and

$$\rho_{(m_t)} = \sum_{\nu}^{\nu_{\text{Fermi}}} |\varphi_{\nu, m_t}|^2 \quad (14)$$

for the self-consistent field model (1) of spherical nuclei. The electromagnetic part is assumed to be given by the static Coulomb potential V_{Coul} of the proton density $\rho_{(-1/2)}$ normalized to $Z-1$; [cf. Eq. (17)].

(1) The parameter v simply determines the energy scale and was adjusted in all computations to give (within 0.3 MeV) the total binding energy for Pb^{208} .

(2) According to the discussion in Sec. 1 B, the non-locality range should be $0.7 \lesssim a \lesssim 0.9$ fm. An increase in a widens the level spacings, i.e., decreases the effective

³³ P. C. Sood and H. G. Leighton, Nucl. Phys. 111A, 209 (1968).

³⁴ K. A. Brueckner, J. L. Gammel, and H. Weitzner, Phys. Rev. 110, 431 (1958).

³⁵ J. B. Law and D. W. L. Sprung, in Proceedings of the 1968 International Symposium on Nuclear Structure, Dubna, USSR (unpublished).

³⁶ Cf. for example, V. A. Chepurnov and P. E. Nemirowsky Nucl. Phys. 49, 90 (1963).

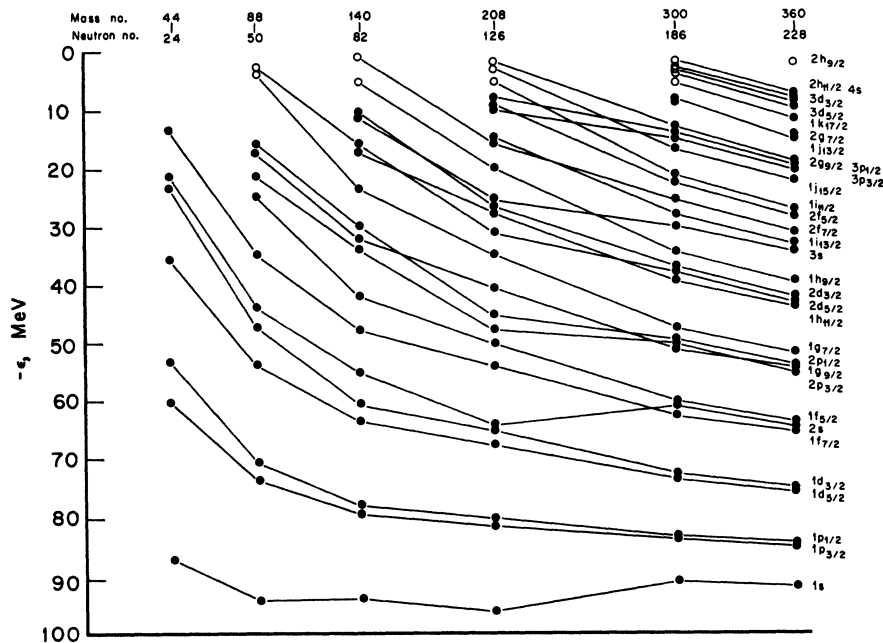


FIG. 3. Neutron eigenvalue spectra; cf. Fig. 2.

nucleon mass—as is readily seen from Eqs. (4) and (5). An increased a yields larger rms radii if v is decreased according to (1) and all other parameters are kept fixed (cf. the discussion below on parameter set B).

(3) The parameter ρ_1 stands for the (average) critical nucleon density where the nucleon-nucleus interaction changes from attractive to repulsive. Since actual nuclei saturate with (average) central densities around 0.15 fm^{-3} , ρ_1 must be larger than this value. An upper limit around 0.5 fm^{-3} is given from hard sphere packing according to hard-core NN potential models. It turns out that the present model reproduces the rms radii of actual nuclei for $0.2 < \rho_1 \lesssim 0.4 \text{ fm}^{-3}$.

(4) The observed sequence of shell closures allows a fairly unique determination of the strength σ for the conventional spin-orbit term. This parameter is confined here to $0.45 \lesssim \sigma \lesssim 0.55 \text{ fm}^2$ if one wants to reproduce the magic nucleon numbers up from $N = Z = 20$. Of course, even narrower limits result if the other

parameters are kept fixed and/or further details of the shell-model spin assignments are required.

(5) The isospin mixing parameter τ determines (like σ) essentially some sort of fine structure; e.g., the isotope shifts in rms radii. Satisfactory fits to most gross data, like masses and radii, are possible with a very wide range of τ values. But in order to fit the isotope mass dependences as well as rms dependences and the neutron/proton ratios in heavy nuclei, this parameter should be in the range $0.1 < \tau \lesssim 0.5$.

The above discussion reveals the problem of a fit here; there are various data of different dimensions that should be reproduced reasonably well. But within the scope of this work there is no apparent preferable selective principle for a better fit to one particular set of data, fitting-radii at the expense of fitting masses, for example. Naturally, it depends on the application of the model, to which data some sort of least square fit will be performed. In any case, the parameters should be confined to the “physical” limits discussed above.

The parameter set A of Table I was used here for the fairly extensive comparison with data of spherical nuclei. The set B of Table I has the parameters a and ρ_1 close to the limits of their reasonable regions. A decrease in rms radii (by about 4%) that would result because of the increase of ρ_1 from 0.3 to 0.4 fm^{-3} is compensated for in this case by increasing the non-locality from 0.8 to 0.9 fm . Some results for parameter set B are given in Table II.

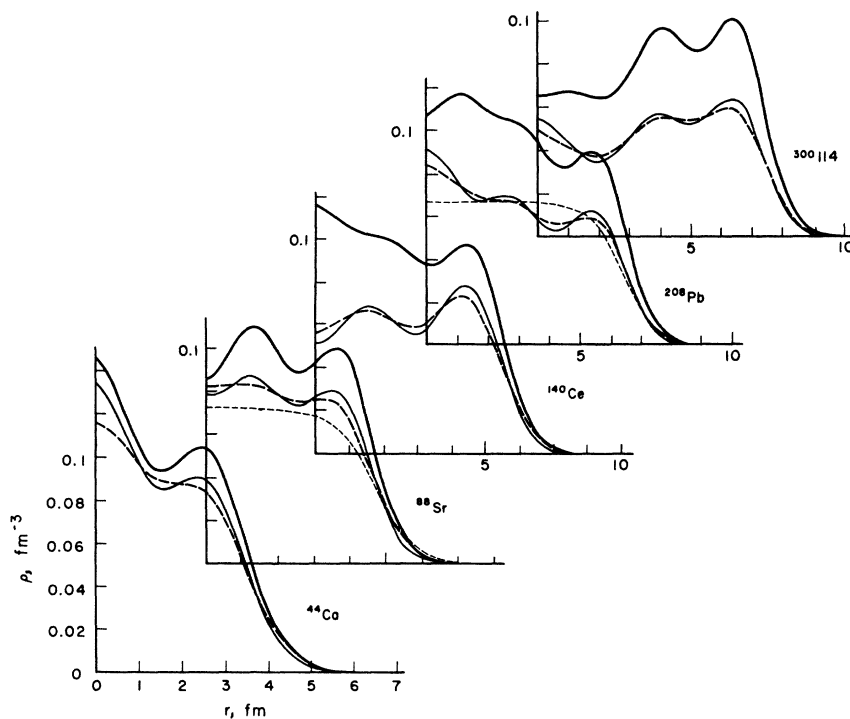
B. Results for a Typical Parameter Set

It should be emphasized that all results in this paper except for Table II refer to computations done with

TABLE II. Some results for parameter set B; cf. Sec. 2 A. For experimental data and the pairing correction see Tables III and V.

	Binding energy (MeV)	$\langle r^2 \rangle^{1/2}_{\text{charge}}$ (fm)
^{44}Ca	396.4	3.18
^{208}Pb	1636.2	5.38
^{209}Bi – ^{208}Pb	4.9	
^{208}Pb – ^{207}Tl	5.7	
^{209}Pb – ^{208}Pb	4.8	
^{208}Pb – ^{207}Pb	5.3	

FIG. 4. Upper and lower solid curves give the density distributions of protons and neutrons for some nuclei on the β stability line. The dashed curves are the nuclear charge densities calculated with Eq. (24) from the corresponding (bare) proton densities. Examples of Fermi function fits to electron scattering data are shown as thin dashed curves. The different fits of Ref. 44 are practically indistinguishable in this figure.



just the one parameter set A of Table I; i.e., everything is computed with simply the rough center values of the above estimated parameter regions. In view of this fact, the general agreement with data throughout the periodic table is surprisingly good. Absolute values for masses, radii, and $1s$ proton levels are reproduced within a few percent. The mass- and radius-difference data are quite satisfactorily reproduced, normally within 30%. Even the higher-order difference quantities such as rearrangement energies or isomer radius shifts seem to result with the correct order of magnitude.

Figure 4 shows density distributions of protons and neutrons (lower and upper solid lines). One point of recent interest is the "neutron skin" of heavy nuclei,³⁷⁻⁴⁰ the Johnson-Teller effect.⁴¹ In the case of ^{208}Pb , for example, the results of pionic scattering and isobaric analog-state analyses seem to disagree significantly with μ or K mesic experiments. There are two percent rms radius differences between neutron and proton densities deduced from the former type of data,^{37,40} whereas a difference of more than 10% is reported from μ^- atoms and K^- capture, as well as from some optical-

and shell-model analyses.³⁸ The present self-consistent model gives $\text{rms}(n) - \text{rms}(p) = 0.07$ fm (see Table III) in excellent agreement with the value 0.07 ± 0.03 fm due to an analysis of the isobaric analog state³⁹ which is consistent with recent $\pi^\pm\text{-Pb}$ scattering data.⁴⁰ In addition, the absolute magnitude of the ^{208}Pb rms charge radius given in Table III agrees perfectly with elastic electron scattering experiments yielding the value 5.42 ± 0.03 fm.⁴² One should notice the neutron

TABLE III. Binding energies and rms radii for some spherical nuclei. Additional comparisons with experimental data give, e.g., for the $1s$ proton level in ^{40}Ca : experimental 77 ± 14 MeV*, calculated 79 MeV.

Nucleus	Binding energy (MeV)		Calculated rms radii (fm)		
	Experimental	Calculated	$\langle r^2 \rangle^{1/2}_{\text{charge}}$	$\langle r^2 \rangle^{1/2}_p$	$\langle r^2 \rangle^{1/2}_n$
^{40}Ca	342.0	339.4	3.15	3.06	3.02
^{44}Ca	380.9	380.3	3.22	3.13	3.20
^{48}Ca	416.1	426.6	3.29	3.20	3.34
^{88}Sr	768.5	777.5	4.02	3.95	4.02
^{118}Sn	1004.8	1017.9	4.50	4.43	4.47
^{140}Ce	1172.8	1189.0	4.74	4.68	4.73
^{208}Pb	1636.4	1636.4	5.44	5.38	5.45
$^{300}114$		2140.5	6.26	6.21	6.24

* Reference 22.

³⁷ D. H. Wilkinson, in Proceedings of the 1968 International Symposium on Nuclear Structure, Dubna, USSR; Comment Nucl. Part. Phys. I, 80 (1967).

³⁸ L. R. B. Elton, Phys. Letters **26B**, 689 (1968); G. W. Greenless, G. S. Pyle, and Y. C. Tang, Phys. Rev. Letters **17**, 33 (1968); B. Holmquist and T. Wiedling, Phys. Letters **27B**, 411 (1968); H. A. Bethe and P. J. Siemens, *ibid.* **27B**, 549 (1968).

³⁹ S. A. Nolen, Jr., J. P. Schiffer, and N. Williams, Phys. Letters **27B**, 1 (1968).

⁴⁰ E. H. Auerbach, H. M. Querski, and M. M. Sternheim, Phys. Rev. Letters **21**, 162 (1968).

⁴¹ Cf. M. H. Johnson and E. Teller, Phys. Rev. **93**, 357 (1954).

⁴² J. Bellicard and K. J. van Oostrum, Phys. Rev. Letters **19**, 242 (1967).

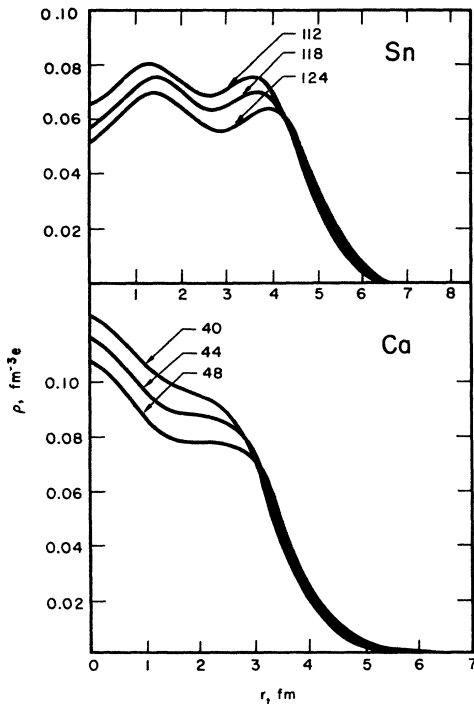


FIG. 5. Isotopic variation of charge density distributions for $^{40,44,48}\text{Ca}$ and $^{112,118,124}\text{Sn}$; cf. Table IV for rms radii.

skin or halo of ^{208}Pb shown in Fig. 4 which looks surprisingly large in view of the small rms radius difference. In the case of ^{40}Ca , the effect is reversed. According to the present calculation, the rms radius of neutrons is 0.04 fm smaller than that of the protons, in qualitative agreement with a recent optical model analysis.⁴³

Figure 5 and Table IV give calculated isotopic variations of charge densities for some Sn and Ca isotopes. For example, the calculated ^{44}Ca to ^{40}Ca rms charge radius difference agrees well with experiments.⁴⁴ Use of the standard $(N-Z)/A$ term from optical-model fits [instead of the term (10)] would yield the wrong sign for this shift.

3. REARRANGEMENT EFFECTS

In any HF-type many-body formalism, the kernels depend on the occupation functions, which are, e.g., for the ground state, $\theta(\epsilon_{\nu p} - \epsilon_{\nu})$ in the HF formalism, and $\frac{1}{2}\{1 + (\epsilon_{\nu p} - \epsilon_{\nu}) / [(\epsilon_{\nu p} - \epsilon_{\nu})^2 - \Delta^2]^{1/2}\}$ in Hartree-Bogoliubov-type formalisms. The effective force acting on a single nucleon will therefore change when different states (orbits) are occupied by the other particles, i.e., when the residual nucleus rearranges. The corresponding *orbital* rearrangement energies have been discussed

⁴³ N. Berovic, P. M. Rudolph, and S. M. Scarrott, Phys. Letters **27B**, 477 (1968).

⁴⁴ K. J. van Oostrum, R. Hofstadter, G. K. Nöldecke, M. R. Yearian, B. C. Clark, R. Herman, and D. G. Ravenhall, Phys. Rev. Letters **16**, 528 (1966); R. D. Ehrlich, D. Fryberger, D. A. Jensen, C. Nissim-Sabat, R. J. Powers, V. L. Telegdi, and C. K. Hargrove, Phys. Rev. Letters **18**, 959 (1967).

with this model in some detail elsewhere.¹⁵ They were shown to be comparable to eigenvalue-differences in local (Woods-Saxon-type) potential wells. Hence, it is an unjustified simplification to identify such *level spacings* with the *mass differences* observed, e.g., in nucleon transfer reactions. Parameter set A of Table I gave a good fit to all difference data in the Ca region. One typical example is the first neutron-hole state for ^{47}Ca : The observed mass difference to the ground state of about 2.6 MeV is reproduced by the present single-particle Hamiltonian that gives at least 6 MeV for the corresponding level spacing; i.e., more than 3.4 MeV result from orbital rearrangement (cf. Ref. 15).

The agreement with the mass data is also excellent for the $^{40}\text{Ca} \pm$ (one nucleon) differences (see Table V). For this example another type of rearrangement effect is revealed in Fig. 6. Conventionally, the eigenvalues were fitted to the experimental total binding energy differences; i.e., rearrangement was totally neglected. Of course, one could not do better in calculations that had no chance to get the right order of magnitude for the total binding—as in *local* potential-model fits. Here, in Fig. 6, the observed binding energy differences are reproduced within 0.2 MeV. However, due to rearrangement, they differ up to 6 MeV from the corresponding eigenvalues.

It might be argued that for some reason this model strongly overestimates rearrangement effects. But the magnitude of this model's rearrangement response can be checked to some extent by a comparison with the calculated isomer shifts due to single-particle excitations (Table VI). Their order of magnitude seems to be confirmed by some relevant data.⁴⁵ This corroborates the present results on rearrangement energies because of the well-known radial and eigenvalue shift correlation for single-particle potential models.

This observation also casts doubts on shell-model calculations that use the observed total binding energy differences (of $A \pm 1$ -nucleon systems) as the eigenvalues for one constant single-particle Hamiltonian. Rearrangement destroys the orthogonality of the wave

TABLE IV. Some calculated isotope shifts of rms radii. Within the accuracy of the calculation, the charge radius differences are equal to the corresponding proton results and the $^{124}\text{--}^{122}\text{Sn}$, $^{122}\text{--}^{120}\text{Sn}$, and $^{118}\text{--}^{116}\text{Sn}$, as well as the $^{116}\text{--}^{114}\text{Sn}$ differences are all equal to the $^{120}\text{--}^{118}\text{Sn}$ shift. Note the large calculated neutron rms radius difference for $^{48}\text{--}^{44}\text{Ca}$.

	$\Delta \langle r^2 \rangle_p^{1/2}$ (fm)	$\Delta \langle r^2 \rangle_n^{1/2}$ (fm)
$^{44}\text{Ca}\text{--}^{40}\text{Ca}$	0.08	0.08
$^{48}\text{Ca}\text{--}^{44}\text{Ca}$	0.08	0.15
$^{120}\text{Sn}\text{--}^{118}\text{Sn}$	0.04	0.06
$^{114}\text{Sn}\text{--}^{112}\text{Sn}$	0.01	0.01

⁴⁵ D. Quitmann, of the Lawrence Radiation Laboratory, University of California at Berkeley (private communication).

TABLE V. Rms radius and binding-energy differences at closed shells±one nucleon for established magic numbers and for $Z=114$. The pairing correction is assumed to be $(15/A^{1/2})$ MeV.^a The energies are calculated with an accuracy of about 0.2 MeV; the radii within about 3×10^{-3} fm. No radius difference is reported for cases where the result was smaller than this error. The calculated charge radius differences agree with the corresponding proton results within the numerical accuracy.

Magic number	Nuclei	Binding-energy differences (MeV)		Calculated radius differences (fm)	
		Experimental	Calculated	$\Delta \langle r^2 \rangle_p^{1/2}$	$\Delta \langle r^2 \rangle_n^{1/2}$
$N=20$	$^{41}\text{Ca}-^{40}\text{Ca}$	8.4	8.4	0.019	0.048
	$^{40}\text{Ca}-^{39}\text{Ca}$	15.6	15.3	0.006	0.005
$Z=20$	$^{41}\text{Sc}-^{40}\text{Ca}$	1.1	1.1	0.051	0.022
	$^{40}\text{Ca}-^{39}\text{K}$	8.3	8.0	0.021	0.011
$N=28$	$^{49}\text{Ca}-^{48}\text{Ca}$	5.0	0	0.010	0.042
	$^{48}\text{Ca}-^{47}\text{Ca}$	10.1	13.3	0.020	0.034
$Z=28$	$^{63}\text{Cu}-^{62}\text{Ni}$	6.1	2.7	0.011	0.003
	$^{62}\text{Ni}-^{61}\text{Co}$	11.1	13.9	0.033	0.017
$N=50$	$^{89}\text{Sr}-^{88}\text{Sr}$	6.8	5.3	0.007	0.013
	$^{88}\text{Sr}-^{87}\text{Sr}$	11.1	11.7	0.004	...
$Z=50$	$^{119}\text{Sb}-^{118}\text{Sn}$	5.2	2.3	0.008	...
	$^{118}\text{Sn}-^{117}\text{In}$	9.9	10.7	0.004	...
$N=82$	$^{141}\text{Ce}-^{140}\text{Ce}$	5.5	3.3	...	0.007
	$^{140}\text{Ce}-^{139}\text{Ce}$	9.1	8.6	0.005	...
$Z=82$	$^{209}\text{Bi}-^{208}\text{Pb}$	3.8	3.3	0.008	...
	$^{208}\text{Pb}-^{207}\text{Tl}$	8.0	5.5
$N=126$	$^{209}\text{Pb}-^{208}\text{Pb}$	3.9	3.2	0.004	...
	$^{208}\text{Pb}-^{207}\text{Pb}$	7.4	5.4	0.004	0.006
$Z=114$	$^{287}\text{115}-^{286}\text{114}$...	0
	$^{286}\text{114}-^{285}\text{113}$...	3.4
	$^{301}\text{115}-^{300}\text{114}$...	0.1
	$^{300}\text{114}-^{299}\text{113}$...	5.2

^a P. E. Nemirowsky and Yu. V. Adamchuk, Nucl. Phys. **39**, 551 (1962); for experimental rms charge radius differences, cf., for example, D. Quittmann, Z. Physik **206**, 113 (1967).

functions for single-particle states of nuclei with different excitations and/or nucleon numbers.

4. MAGIC PROTON NUMBER 114

The charge spectrum of cosmic-ray nuclei indicates the existence of nuclei with $Z \geq 110$.⁴⁶ An increasing

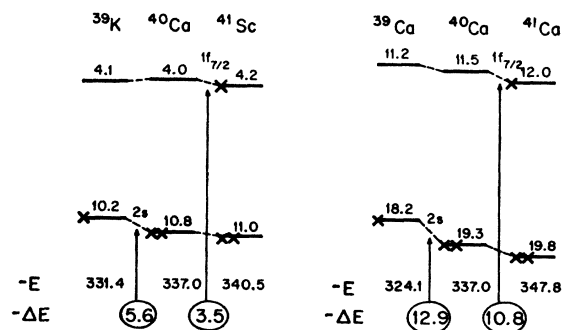


FIG. 6. Example for rearrangement effects: $N=Z=20$ shell±one nucleon. Compare the eigenvalues (in MeV) (arrows) with the circled total binding-energy differences ΔE (also in MeV). An excellent fit to the data results (cf. Table V) when a pairing correction of 2.4 MeV is added to ^{40}Ca . Conventionally, the eigenvalues are identified with total binding-energy differences; cf. Sec. 3.

⁴⁶ P. H. Fowler, University of Bristol, Wills Physics Laboratory Report (unpublished); I am grateful to Professor N. Flerov for drawing my attention to this work.

amount of experimental effort is spent now to produce such superheavy nuclei.⁴⁷ For some time, $Z=126$ was the main theoretical candidate for a relatively stable superheavy nucleus. This belief, based on a simple-minded shell-model picture that did not differentiate between protons and neutrons, thus assumed a repetition of the $N=126$ shell in Z .

Shell closures, i.e., structure-dependent tendencies to prefer spherical shapes, have been shown to be of prime importance for the spontaneous-fission half lives of

TABLE VI. Examples of rms charge radius differences between the first one-neutron-hole excitation and the ground state. Except for the case of Ca, the amount of computer time invested here did not allow checking for more than the orders of magnitude.

	$\Delta \langle r^2 \rangle_p^{1/2}$ (fm)	$\Delta \langle r^2 \rangle_n^{1/2}$ (fm)
$^{47}\text{Ca}^*-^{47}\text{Ca}$	0.012	0.037
$^{207}\text{Tl}^*-^{207}\text{Tl}$	10^{-3}	10^{-3}
$^{207}\text{Pb}^*-^{207}\text{Pb}$	10^{-4}	10^{-3}

⁴⁷ S. G. Nilsson, S. E. Thompson, and C. F. Tsang, Phys. Letters **28B**, 465 (1969); S. G. Thompson, of the Lawrence Radiation Laboratory, University of California at Berkeley (private communication); N. Flerov, in the Proceedings of the 1968 International Symposium on Nuclear Structure, Dubna USSR (unpublished).

superheavy nuclei.¹⁷ The contribution to the barrier height due to shells is negligible at the proton number $Z=50$ and is about 30% of the total for Z around 82 near the β stability line. In the region beyond $Z=110$ the average value, or liquid-drop-model barrier, becomes practically negligible, since it is quite small as compared to the present uncertainties about structure-dependent contributions there.

About four years ago, calculations of this author showed $Z=114$, $N=184$ to be a clearly preferable candidate for a rather stable superheavy nucleus.¹⁶ This has since been confirmed by many independent computations^{14,18} and is widely discussed now.⁴⁸ The extrapolations were based on single-particle potential fits that showed a shell structure in the eigenvalues similar to the one observed in the experimental mass defects. Fluctuating rearrangement effects were totally neglected. Most authors used the questionable procedure of identifying eigenvalue spacings with mass differences (cf. Sec. 3).

The present calculations check the real shell effects in the nuclear masses. As can be seen from Table V, the partial derivative $\partial E/\partial Z$ of the total binding energy (mass) changes considerably at the proton number $Z=114$ when parameter set A of Table I is used for superheavy nuclei. The present calculations for $N=172$ and 186 show the expected decrease of the shell effect for isotopes far from the extrapolated beta stability line. At $N=172$ and $Z=114$, the lack of neutron excess seems to smooth the step in the mass function to an insignificant wiggle. For 186 neutrons the shell effect has the magnitude observed at established magic numbers. Therefore, experiments on $Z=114$ should aim for compound nuclei with mass numbers around 290 or higher.

5. DEFORMED NUCLEI AND FISSION

It is rather straightforward to extend the model given by Eqs. (1), (13), and (14) to nonspherical, in particular axially symmetric, density distributions. Present computer sizes, however, seem to require some sort of "local energy approximation" to the nonlocality problem. For this case, most aspects of the resulting numerical work have been investigated recently.⁴⁹ The present Hamiltonian is, in such an approximation for axial symmetric cases (cf. Ref. 49, Eq. 2.8),

$$H_{m_i} = (\mathbf{p}^2/2m) + v(\epsilon_{r,m_i}) \{1 - [\rho_{m_i}(z, b)/\rho_1]^{2/3}\} \\ \times [1 - (\sigma/\hbar)(\mathbf{p} \times \mathbf{s}) \cdot \nabla] \rho_{m_i}(z, b) + (\frac{1}{2} - m_i)V_c(z, b), \quad (15)$$

where cylinder coordinates (z, b) are introduced,

⁴⁸ A. M. Weinberg, *Phys. Today* **20**, 23 (1967); C. Y. Wong, *Phys. Rev. Letters* **19**, 328 (1967); see also G. T. Seaborg, *Ann. Rev. Nucl. Sci.* **18**, 53 (1968).

⁴⁹ F. Dickmann, *Z. Physik* **203**, 141 (1967).

$b^2 = x^2 + y^2$, and ρ_{m_i} is the effective density calculated according to Eqs. (13) and (14). Two methods are mainly used for the computation of the energy-dependent local potential that corresponds to a given Van Vleck-type kernel. In bound-state calculations the simple technique of using the Fourier transform according to Eqs. (4) and (5)

$$v(\epsilon) = \{1 + (2m/\hbar^2)a^2[\epsilon - v(\epsilon)]\}^{-1} \quad (16)$$

is probably as good⁵⁰ as the fancier LEA.⁵¹ Equations (15) and (16) give a framework for self-consistent calculations of nuclear single-particle data. The problematic boundary condition of "volume conservation" in equipotential contours, for example, is completely avoided here. In fact, most of the classical difficulties⁵² of the Nilsson-type models for deformed nuclei and adiabatic fission computations do not arise.

6. CONCLUSIONS

The final remarks of Sec. 5 reveal the main reason for the computations done so far, namely, a check of the qualities of the proposed model that is designed to work for a much wider range of applications. Already here, the proposed Hamiltonian was used for the calculation of more independent data than was conceivable with previous models. For spherical nuclei, one constant set of five physical parameters allowed satisfactory reproduction of

- (1) charge density distributions, including isotope and isomer shifts,
- (2) $1s$ proton levels as measured in $(e, e'p)$ scattering,
- (3) total binding energies of nuclear mass defects, and
- (4) the shell-model spin assignments and mass structure

throughout the periodic table. Hence, it seems that all future work in this direction has to confirm *quantitatively* the essential features of a nuclear kernel determined here, particularly the *nonlocality* and *rearrangement* effects. The present concept works quantitatively well enough to allow predictions such as the proton shell 114.

Equation (1) was solved (numerically) exactly. The results can therefore be used to check approximations that might be necessary for deformed and fissioning nuclei.

Naturally, there are many improvements to be considered, such as those mentioned in the discussion

⁵⁰ M. Krell, *Z. Physik* **205**, 272 (1967).

⁵¹ Cf., for example, H. Meldner and G. Suessmann, *Z. Naturforsch.* **20a**, 1217 (1965); H. Fiedeldey, *Nucl. Phys.* **77**, 149 (1966).

⁵² L. Wilets, *Theories of Nuclear Fission* (Clarendon Press, Oxford, England, 1964), Chap. 4.3.

about the spin-orbit term. Some residual interaction effects of the pairing type, for instance, could be taken into account by appropriately smoothing the step function used in Eq. (14) for the occupation probability distribution.

atory and of the University of California Physics Department. I am indebted to many members of both institutions for helpful discussions. This lengthy investigation would have been impossible without the generous support of Professor S. G. Thompson.

ACKNOWLEDGMENTS

I would like to acknowledge the hospitality of the University of California Lawrence Radiation Labor-

APPENDIX

For spherical symmetric density distributions the radial equation is

$$\begin{aligned} [(\hbar^2/2m)\{d^2/dr^2 - [l(l+1)/r^2]\} - \epsilon_{nljm_i}]u_{nljm_i}(r) = v \int_0^\infty dr' h_l(r, r') \{1 - [\rho_{m_i}(x)/\rho_1]^{2/3}\} \\ \times \{\rho_{m_i}(x) - (\sigma/2x)[j(j+1) - l(l+1) - \frac{3}{4}]\rho'_{m_i}(x)\} u_{nljm_i}(r') \\ + (\frac{1}{2} - m_i)((Z-1)/Z)e^2 \left[r^{-1} \int_0^r dr' r'^2 \rho_{(-1/2)}(r') + \int_r^\infty dr' r' \rho_{(-1/2)}(r') \right] u_{nljm_i}(r), \end{aligned}$$

where $x = \frac{1}{2}(r+r')$, n denotes the radial, l denotes the orbital-angular momentum, j denotes the total-angular-momentum quantum number, and m_i denotes the isospin 3-component for the nucleon in question; ρ' is the derivative of ρ with respect to the argument and $e^2 = 1.4368$ MeV fm. The h_l are the partial-wave projections of the width function $v(|\mathbf{r}-\mathbf{r}'|)$.

The single-particle equation is assumed to emerge from pure two-body internucleon forces. The total binding energy is therefore

$$E = \sum_i t_i - \frac{1}{2} \sum_{i,j} u_{ij} = \frac{1}{2} \sum_i \left[\epsilon_i + \int d\mathbf{r} \varphi_i^*(\mathbf{r}) t(\mathbf{r}) \varphi_i(\mathbf{r}) \right], \quad (18)$$

where the sums extend over the occupied levels; t_i is for the spherical cases

$$t_{nljm_i} = (\hbar^2/2m) \int_0^\infty dr \{ [l(l+1)/r^2] u_{nljm_i}^2(r) + (r(d/dr)[u_{nljm_i}(r)/r])^2 \}. \quad (19)$$

Eigenstates in Strongly Nonlocal Potentials

The computer problem is to find the first few eigenvalues e and eigenvectors u of an integrodifferential equation

$$\{(d^2/dr^2) - [e + C(r)]\}u(r) + \int_0^\infty dr' g(r, r')u(r') = 0 \quad (20)$$

for boundary conditions of the type $\lim_{r \rightarrow 0} u(r) \sim r^{l+1}$ and $\lim_{r \rightarrow \infty} u(r) \sim \exp[-r(e)^{1/2}]$. Selecting an appropriate finite integration interval $(0, R)$ divided into N parts and with $s = R/N$, $c_i = C(is)$, and $g_{ij} = g(is, js)$, one gets the corresponding difference equation $(h - e)u = 0$ with a symmetric matrix

$$h = \begin{pmatrix} sg_{11} - C_1 - 2/s^2 & sg_{12} + 1/s^2 & sg_{13} & \cdots & sg_{1N} \\ sg_{21} + 1/s^2 & sg_{22} - C_2 - 2/s^2 & & & \\ sg_{31} & & & & \\ \vdots & & & & \\ sg_{N1} & & & & sg_{NN} - C_N - 2/s^2 \end{pmatrix}.$$

A good approximation $u^{(0)}$ to u is obtained, e.g., from a LEA program.⁵¹ The vector $u^{(0)}$ fulfills approximately the same boundary conditions as u and has the same number of nodes. An appropriate iteration program is the following:

Start with $i=0$.

- (1) Normalize by replacing $u^{(i)}$ with $u^{(i)}(1/u^{(i)T}u^{(i)})$.
- (2) Compute $e^{(i)} = u^{(i)T}hu^{(i)}$.
- (3) Solve $u^{(i+1)} = (h - e^{(i)})^{-1}u^{(i)}$ with some standard inversion program.⁵³
- (4) Replace i with $i+1$; go to (1) unless $|e^{(i+1)} - e^{(i)}|/|e^{(i)}| \ll 1$.

This "Wielandt inverse iteration"⁵⁴ works as follows: Let v be the exact solution, i.e., $(h - e_m)v_m = 0$. Then, step (3) is in spectral decomposition

$$\begin{aligned} \sum c_m^{(i+1)}v_m &= (h - e^{(i)})^{-1} \sum c_m^{(i)}v_m \\ &= \sum_m [c_m^{(i)} / (e_m - e^{(i)})]v_m, \end{aligned} \quad (21)$$

so that

$$c_m^{(i+1)} = c_m^{(i)} / (e_m - e^{(i)}).$$

Therefore, the iteration converges to the nearest eigenvector v_m which is picked out via the above pole.

Partial-Wave Projections of Yukawa Functions

The above h_l are

$$h_l(r, r') = 2\pi r r' \int_{-1}^1 dz P_l(z) \frac{e^{-|r-r'|/a}}{|r-r'|/a},$$

with $r = |\mathbf{r}|$, $z = \mathbf{r}\mathbf{r}'/rr'$, since⁵⁵

$$\begin{aligned} &\frac{\exp[-(1/a)(r^2 + r'^2 - 2rr'z)^{1/2}]}{(r^2 + r'^2 - 2rr'z)^{1/2}} \\ &= \sum_{l=0}^{\infty} (2l+1) P_l(z) (rr')^{-1/2} K_{l+1/2}(r'/a) I_{l+1/2}(r/a), \end{aligned}$$

one has

$$h_l(r, r') = 4\pi a (rr')^{1/2} I_{l+1/2}(r/a) K_{l+1/2}(r'/a) \quad \text{for } r < r'.$$

⁵³ E.g., the Fortran routine LIMIT of the Lawrence Radiation Laboratory, University of California at Berkeley, Computing Center.

⁵⁴ H. Wielandt, Report No. B44/J/37, Aerodyn. Vers.-Anstalt Göttingen, 1944 (unpublished); J. H. Wilkinson, *The Algebraic Eigenvalue Problem* (Clarendon Press, Oxford, England, 1965), p. 321.

⁵⁵ G. N. Watson, *Theory of Bessel Functions* (University Press, Cambridge, England, 1962).

Also from Ref. 55, p. 80,

$$\begin{aligned} I_{l+1/2}(x) K_{l+1/2}(x) &= \frac{1}{2} (xx')^{-1/2} [e^x \sum_{k=0}^l (-)^k T_{lk}(x) \\ &\quad - (-)^l e^{-x} \sum_{k=0}^l T_{lk}(x)] e^{-x'} \sum_{k=0}^l T_{lk}(x'), \end{aligned}$$

with $T_{lk}(x) = (l+k)! / (k!(l-k)!(2x)^k)$. The following formula is feasible for computations:

$$\begin{aligned} h_l(r, r') &= 2\pi a^2 [e^{r/a} \sum_{k=0}^l (-)^k T_{lk}(r/a) \\ &\quad - (-)^l e^{r'/a} \sum_{k=0}^l T_{lk}(r/a)] e^{-r'/a} \sum_{k=0}^l T_{lk}(r'/a) \end{aligned}$$

for $r < r'$, (22)

so that $h_0(r, r') = 2\pi a^2 (e^{r/a} - e^{-r/a}) e^{-r'/a}$, etc.

Charge Density and Proton Form Factors

The nuclear charge density ρ_{ch} is obtained by folding the proton probability distribution with the electric proton form factor f

$$\rho_{ch}(\mathbf{r}) = \sum_{\nu} \int d\mathbf{r}' |\varphi_{\nu,-1/2}|^2 \cdot f(|\mathbf{r} - \mathbf{r}'|). \quad (23)$$

The $\varphi_{\nu,-1/2}$ are properly normalized single-particle wave functions and the sum extends over all occupied proton levels. The best phenomenological proton form factor appears to be an exponential⁵⁶

$$f(r) = (\alpha^3/8\pi) e^{(-\alpha r)},$$

with

$$\alpha = (12/\langle r^2 \rangle)^{1/2} \quad \text{and} \quad \langle r^2 \rangle = \int d\mathbf{r} r^2 f(r).$$

For spherical symmetric $\rho = \sum |\varphi|^2$ one has

$$\begin{aligned} \rho_{ch}(r) &= (\alpha/4r) \int_0^{\infty} dr' r' \rho(r') [(\alpha|r-r'|+1)e^{-\alpha|r-r'|} \\ &\quad - [\alpha(r+r')+1]e^{-\alpha(r+r')}]. \end{aligned} \quad (24)$$

The present calculations were done with the value $\langle r^2 \rangle^{1/2} = 0.75$ fm (cf. Ref. 56).

⁵⁶ F. Burmiller, M. Croissiaux, E. Dally, and R. Hofstadter, *Phys. Rev.* **124**, 1623 (1961); for a comparison with other form factors see P. Hofstadter, *Rev. Mod. Phys.* **30**, 482 (1958).